Fusion Engineering and Design 128, 2018

https://doi.org/10.1016/j.fusengdes.2018.01.045

Integrated Plasma Control for Long Pulse Advanced Plasma Discharges on EAST

B.J. Xiao[1,2*], Z.P. Luo[1], Q.P. Yuan[1], K. Wu[1], Y. Guo[1], Y.H. Wang[1], G. Calabrò[3], F. Crisanti[3], R. Albanese[4], R. Ambrosino[4], G. De Tommasi[4], F. Crisanti[3], Y. Huang[1], D.A. Humphreys[5]

[1]Institute of Plasma Physics, Chinese Academy of Sciences, Hefei, 230031, China
[2]School of Nuclear Science and Technology, University of Science and Technology of China, Hefei 230031, China
[3]*ENEA Unità Tecnica Fusione, C.R. Frascati, Via E. Fermi 45, 00044 Frascati, Roma, Italy*
[4]*CREATE, Universittà di Napoli Federico II, Universittà di Cassino and Universittà di Napoli Parthenope, Via Claudio* 19, 80125, Napoli, Italy
[5]General Atomics, DIII-D National Fusion Facility, San Diego, CA, USA
*bjxiao@ipp.ac.cn

For long pulse or steady-state advanced plasma discharges, it is necessary to keep plasma parameters such as plasma shape, loop voltage, plasma pressure in a steady state way. In particular, the heat load on the divertor must be effectively reduced. By using Low Hybrid Wave (LHW) for the current drive, loop voltage has been feedback controlled while plasma current was controlled by the PF coil current. The control of the plasma pressure has been demonstrated by using LHW. Heat load reduction has been done by radiation and advanced shape configuration. By using impurity seeding with gas puff for the feedforward and Super-Sonic Molecular Beam Injection (SMBI) to feedback the total radiation, radiation can be effectively controlled with slight influence to the core confinement. We extended the quasi-snowflake (QSF) discharge to H-mode. It is verified again in H-mode operation, heat load can be effectively reduced under the QSF shape. All these new control algorithms give rise to more assistances to the EAST long pulse operation.

Keywords: Long pulse operation; heat load control; non-inductive current drive; quasi-snowflake divertor;

1. Introduction

For the steady state operation of a tokamak reactor, all the plasma parameters including the shape, pressure and flux must be kept at a certain level, moreover, high divertor heat flux is still a problem for an advance tokamak operation and must be effectively reduced. For EAST, one of the main mission is to demonstrate the long pulse up to steady state operation under high plasma performance [1]. Until 2014, there have been on EAST in total 30 MW power for auxiliary heating and current drive which includes radio frequency wave heating and neutron beam injection. These heating powers together make EAST own the sufficient capability for the advanced plasma performance and current drive for long pulse operation. Therefore, the active control of the heat load as well as control the plasma shape and parameters must be implemented.

For the heat load reduction, there are several options. One is to use the radiation in the edge region to spread more power to the first walls and mitigate the total heat load over the divertor target [2], in particular the narrow region near the divertor strike points. Another way is to use alternative plasma shape configuration. It has been verified the heat reduction capability by using so called snowflake (SF) divertors [3] on most advanced tokamaks such as TCV [4], NSTX [5] and DIII-D [6]. In 2014, we also demonstrated the effects of applying QSF plasma shape [7]. It was found that in L-mode case the peak heat flux to the divertor target can be effectively reduced to at least by a factor of 1/2.

In 2016 campaign, we successfully achieved the radiation control by using divertor gas puff together with mid-plane SMBI. We also extended the QSF operation to the H-mode and upper single null (SN). These heat load reduction methods will be firstly reported and then other recently implemented plasma control algorithm such as plasma pressure control, loop voltage control, which are important for the long pulse high performance plasma operation, will be presented in this paper.

2. Divertor heat load control

By increasing the radiation in the scape-off layer region, the power transferred from core plasma to the edge region can be spread to wider area such as the first wall before reaching the divertor target. This can be done by injection of impurity gas such as Neon, Argon or Nitrogen. The most effective way is to inject the impurity gas from the divertor target or dome region because this would directly reduce the temperature of the plasma in front of the target with less influence to the core plasma. However, due to the long tube connecting the gas valve, latency is unavoidable on EAST. For EAST gas puff, this latency is up to ~ 200 ms, which makes the feedback control by gas puff impossible as we learned this from 2012 experiments.

The radiation can be measured by absolute extreme ultraviolet (AXUV) [8]. In EAST, we have in total 64 lines of chords AXUV which cover edge and core plasma regions. If desired, such arrays can be used for the radiation distribution reconstruction. The detail measurements and control implementation can be found in [9], we showed the control results in Fig.1. From 3s, Neon gas was puffed from the upper divertor target area for a duration of about 20 ms. This increased the total radiation power to a level at about 700 kW. From 4s, we turned on the feedback control by using the mid-plane Neon SMBI. The radiation target was set to 800 kW. It can be seen that the total radiation can be maintained and the influence to the core plasma is slight as one can see that the change of stored energy, shown as W_{MHD} in Fig.1, is negligible after SMBI was turned on.

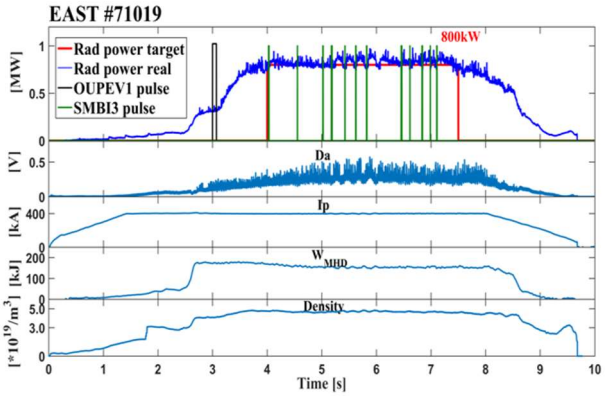

Fig.1 Radiation feedback control by using divertor Neon gas puff and mid-plane Neon SMBI.

It is proving in reference [7] if controlling the plasma shape to the lower single null quasi-snowflake shape (LQSF), the peak heat load can be reduced to the level of a factor below 1/2 in comparision to the conventianl SN diverted plasma configuration. We further extended this operation to exactly control the shape. The shape control algorithms is the same with the SN control algorithms which were reported in [10]. The controllers must be changed as the plasma coupling to each coil is different. We also extended the shape configuration in upper QSF. Shown in right hand side of Fig.2 is the typical lower and upper QSF shapes in 2016 campaign. For the shape feedback in LQSF, in order to control the flux expansion to form the QSF configuration, segments 8 and 9 must be relaxed for non-feedback control. This allows PF coil 6 and 12 to be controlled by the pre-programed (or feedforward) coil currents plus the plasma current feedback requested. In this way, the flux expansion or the secondary X point was roughly controlled. If the pulse period is non-inductive or zero loop voltage, then these 2 coil currents exactly follow the feedforward currents. The typical shot is 70326 for lower QSF. For the upper QSF, the PF coils 5 and 11 are controlled in the same way. The typical shot is 70860. The discharge waveforms of plasma current (I_p), line-averaged line density (n_e) and radial (R) and vertical (Z) positions are also shown in the left hand side of Fig.2. In case of either lower QSF or upper QSF, we used the RZIP (plasma positions R and Z, and current I_p) from 0.2s after plasma starts up to 2.7s to gradually form the QSF shape, which was controlled by the pre-designed PF coil current from a static equilirium calculation together with the estimated shape, position and flux evolution. We have to say that up to now, the operation in QSF is only limited to plasma current as 250 kA. A calculation showed that the limitation of the EAST PF coil current saturation can't allow plasma current higher than 250 kA if it is SF shape. QSF diverted configuration mitigate this PF requirement, however, at the phase for testing the QSF possibility, we selects the level of plasma current at 250 kA for sake of the safer operation. From 2.7 s, the QSF shape is reached and a transition was made to RTEFIT/ISOFLUX or PEFIT/ISOFLUX control algorithms to main the shape. It should be noted that in most of the experiment shots up to now, flux expansion or secondary X points has not been feedback controlled except some lower QSF shots were controlled in SVD(single value de-composition) MIMO (multi-input and multi-output) method which feedback controlled the shape together with the flux expansion or the secondary X point outside the first wall. For this MIMO, the accurate recontruction of the flux expansion or the secondary X point requires finer grid which can not been done by RTEFIT [11], we used PEFIT [12] which is faster and more accurate and meets the demands for the real time reconstruction. Details of PEFIT can be found in [12, 13] and real time implementation with IOSFLUX in EAST PCS can be found in [14]. Detailed implementation of this MIMO algorithm can be found in [15]. Because of the limited machine time, this MIMO algorithm hasn't been matured to a level for the physical experiment, all the results reported in this paper were not controlled in this MIMO way.

At shot 70391, we achieved the H-mode operation under LQSF shape by injecting 0.3 MW electron cyclotron range wave (ECR), 0.5 MW ion cyclotron range frequency wave (ICRF), 1.5 MW neutral beam and 2 MW low hybrid wave, which are shown in the bottom frame of the left hand side of Fig.3. Above this heating power frame, they are frame with core and edge radiations , frame with store energyW_{MHD}, normailized plasma pressureβ_P and confinement factor H_{98}, and the frame of the line averaged electron density $\bar{n}_e$ and edge D_α and the frame with plasma current I_P and loop voltage V_{Loop} in conseqence. The top left part is the results for the conventional lower SN (LSN) arranged in the same order. It can be seen all the plasma

performances including the confinement shown quite similar for both shape unless the D_α ELMy spike in LQSF is smaller. This is reasonable and consistent with what were reported in other advanced tokamak due to the enhanced flux expansion. The heat load on the lower divertor can be reduced from the infrared camera image and the peak fluxes on the divertor target are shown in the bottom part of Fig.3. It can be seen that the peak heat load is reduced to ~2/3 of that in conventional LSN shape. It should be noted that in latter case, ICRF power was missing. In the top middle part of Fig.3, we also showed the LQSF shape and the dedicated conventional shape for comparison. The shape difference is slight, and more machine time is needed if one would want to match more closely because the conventional LSN shape was controlled with so-called biased double null algorithm without effective control of the upper squareness and the LQSF shape was controlled without effective control of the lower squareness.

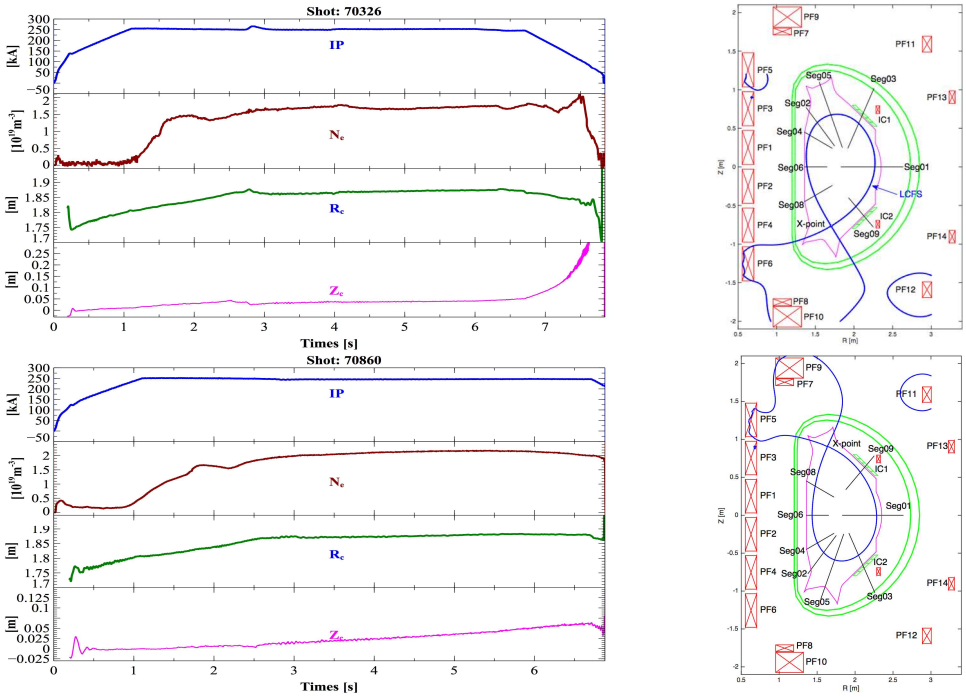

Figure 2 The shape control logics and the discharge scenario to achieve the QSF configurations

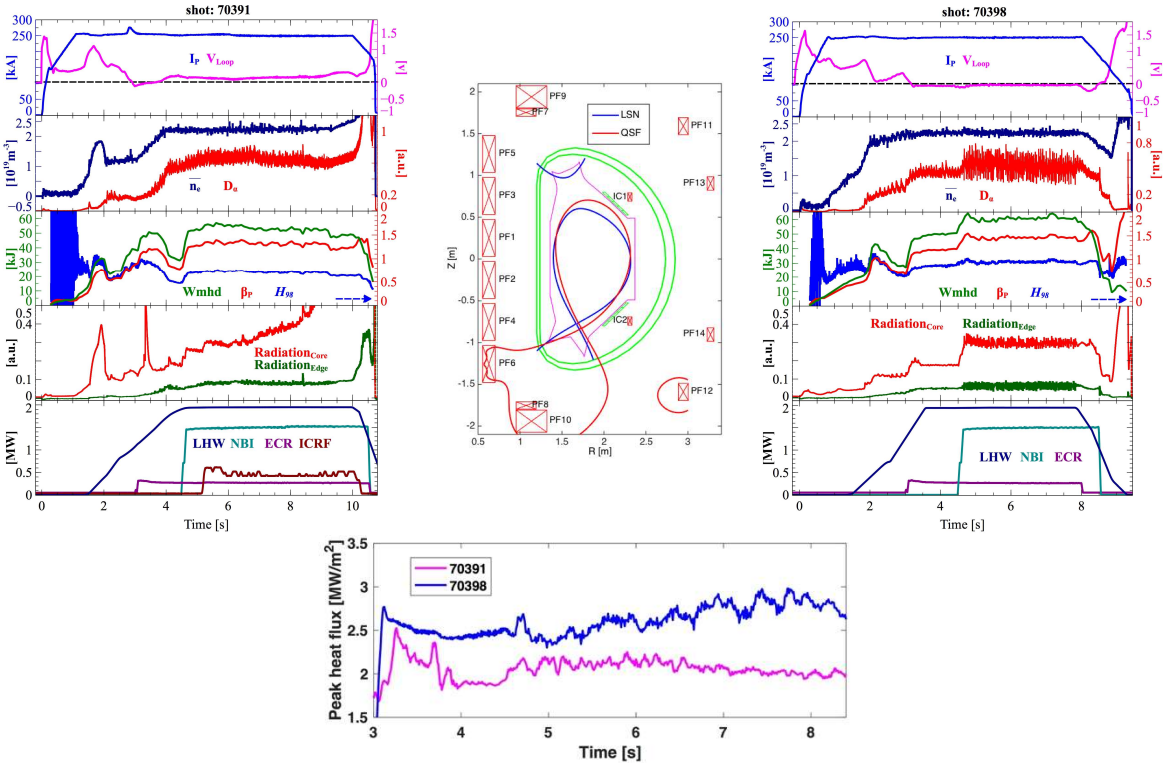

Fig. 3 The results of H-mode operation of the plasma in lower QSF shape (shot 70391) in comparison with those in conventional lower single null shape (shot 70398).

To demonstrate the steady operation of H-mode plasma in LQSF shape, we extended the pulse up to 18 s in shot 70426 as shown in Fig.4. From the top to the bottom frames, plasma current with loop voltage, stored energy with normal pressure and confinement factor, and the heating power are shown. It can be seen that the confinement factor H_{98} was kept above 1 after LHW reached above 1.5 MW at 4.5 s. After this moment, the loop voltage became less than or nearly 0 before plasma ramped down. The steady state with fully non-inducted current drive lasted at least 15 seconds which is much greater than 400 times of the plasma confinement time. For the upper QSF operation, we achieved even more reliable control of the shapes. The detailed report of the upper QSF results can be found in [16].

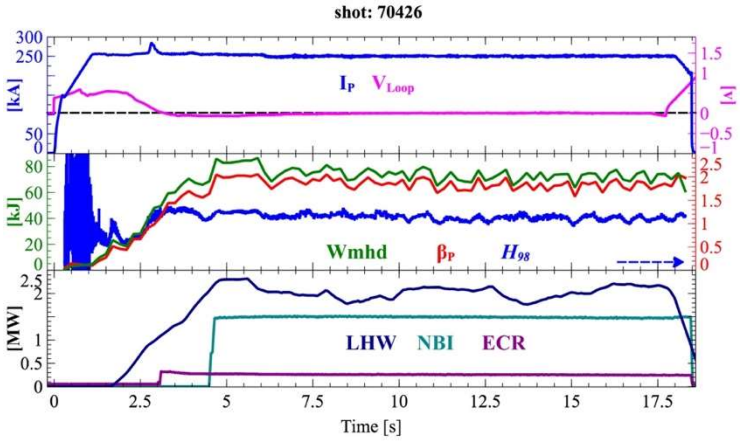

Fig. 4 Steady state H-mode plasma in lower QSF shape

4. Loop voltage and plasma pressure control

Long pulse operation needs efficient current drive to save flux and moreover, the steady state operation needs the plasma current to be fully driven by the external current drive other than Ohmic current drive provided by PF coil system. On EAST, the most efficient current drive is to use LHW. In order to control the heating and current drive, we put dedicated computer, which connects EAST plasma control system by reflected memory network, on each power source end for the interface which sends the commands and receives the power source signals as well. The control detail implementation can be found in [17].

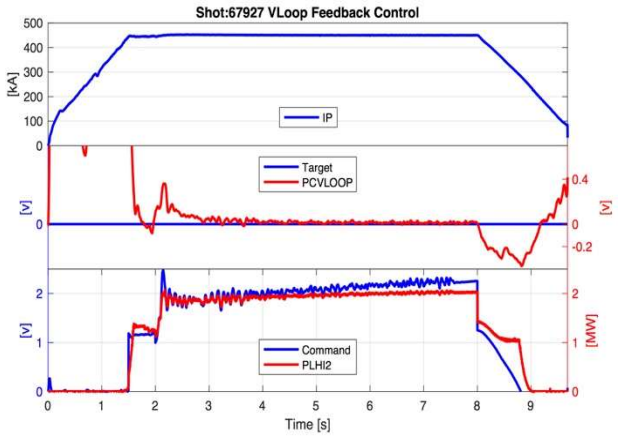

Fig. 5 Loop voltage feedback control by LHW

Figure 5 shows the loop voltage control results, the plasma current, the target and measured (PCVLOOP which is differential flux acquired for the flux loop located on the inner mid-plane) loop voltage, and the command together with actual output of LHW power from the top to the bottom. The loop voltage was controlled by a PI controller with additional feedforward part. At shot 67927, feedback control started from 3.5 s and it can be seen that the loop voltage is almost kept at zero before the plasma ramp down with slightly increased request to the LHW power. In general, the LHW follows the PCS command well and more accurate LHW response could be improved in the future.

For the plasma pressure or β control, the control can be done in the similar way with loop voltage control. β_p can be calculated from RTEFIT or PEFIT reconstruction and the power actuator can be linear combination of the LHW, ECR, ICRF and NBI powers. At shot 67924, we only demonstrated the control algorithm by using LHW although it is not the effective power source to control plasma pressure. This is because the other heating sources are not yet ready to be controlled by PCS.

5. Summary

In 2016 campaign, we implemented and tested the radiation, loop voltage and plasma pressure control. This will assist the long pulse operation under high performance. In particular, we achieved non-inductive plasma operation under the QSF shape. With QSF shape, the heat load reduction is significant although the plasma current is not high and the flux expansion hasn't been well controlled. In the following campaigns, we will actively control the QSF shape together with the flux expansion. To explore the operation window including increase of the plasma current under QSF shape is another mission. Then, to integrate all these control

algorithms together in a long pulse discharge must establish a powerful basis for EAST operation.

Acknowledgments

This work is supported by the National Magnetic Confinement Fusion Science Program of China (Grant No: 2014GB103000) and National Natural Science Foundation of China (Grant No: 11575245).

References

1. Li, J., et al., *A long-pulse high-confinement plasma regime in the Experimental Advanced Superconducting Tokamak.* Nature Physics, 2013. **9**(12): p. 817-821.
2. Loarte, A., et al., *Chapter 4: Power and particle control.* Nuclear Fusion, 2007. **47**(6): p. S203-S263.
3. Ryutov, D.D. and V.A. Soukhanovskii, *The snowflake divertor.* Physics of Plasmas, 2015. **22**(11): p. 110901.
4. Reimerdes, H., et al., *Power distribution in the snowflake divertor in TCV.* Plasma Physics and Controlled Fusion, 2013. **55**(12): p. 124027.
5. Soukhanovskii, V.A., et al., *"Snowflake" divertor configuration in NSTX.* Journal of Nuclear Materials, 2011. **415**(1): p. S365-S368.
6. Soukhanovskii, V.A., et al., *Radiative snowflake divertor studies in DIII-D.* Journal of Nuclear Materials, 2015. **463**: p. 1191-1195.
7. Calabrò, G., et al., *EAST alternative magnetic configurations: modelling and first experiments.* Nuclear Fusion, 2015. **55**(8): p. 083005.
8. Yanmin, D., et al., *Measurement of Radiated Power Loss on EAST.* Plasma Science & Technology, 2011. **13**(5): p. 546-549.
9. Wu, K., et al., *Achievement of radiative feedback control for long-pulse operation on EAST tokamak.* 2017: submitted to Nuclear Fusion.
10. Yuan, Q.P., et al., *Plasma current, position and shape feedback control on EAST.* Nuclear Fusion, 2013. **53**(4): p. 043009.
11. Ferron, J.R., et al., *Real time equilibrium reconstruction for tokamak discharge control.* Nuclear Fusion, 1998. **38**(7): p. 1055.
12. Yue, X.N., et al., *Fast equilibrium reconstruction for tokamak discharge control based on GPU.* Plasma Physics and Controlled Fusion, 2013. **55**: p. 085016.
13. Huang, Y., et al., *Implementation of GPU parallel equilibrium reconstruction for plasma control in EAST.* Fusion Engineering and Design, 2016. **112**: p. 1019-1024.
14. Xiao, B., et al., *Enhancement of EAST plasma control capabilities.* Fusion Engineering and Design, 2016. **112**: p. 660-666.
15. Guo, Y., et al., *Preliminary results of a new MIMO plasma shape controller for EAST*, in *11th IAEA Technical Meeting on Control, Data Acquisition, and Remote Participation for Fusion Research*. 2017: Greifswald, Germany.
16. Xiao, B.J., et al., *A high-confinement steay-state plasma with quasi-snowflake magnetic configurations in EAST tokamak*. 2017: in preparation to submit.
17. Yuan, Q.P., *Upgrade of EAST plasma control system for steady-state advanced operation*, in *11th IAEA Technical Meeting on Control, Data Acquisition, and Remote Participation for Fusion Research*. 2017: Greifswald, Germany.